



Note

Angular momentum conservation in a simplified Venus General Circulation Model

C. Lee*, M.I. Richardson

Ashima Research, Suite 104, 600 South Lake Ave., Pasadena, CA 91101, USA

ARTICLE INFO

Article history:

Received 28 August 2012

Revised 3 October 2012

Accepted 15 October 2012

Available online 24 October 2012

Keywords:

Venus

Venus, Atmosphere

Atmospheres, Dynamics

ABSTRACT

Angular momentum (AM) conservation and transport are critical components of all General Circulation Model (GCM) simulations, and particularly for simulations of the Venus atmosphere. We show that a Venus GCM based upon the Geophysical Fluid Dynamics Laboratory (GFDL) Flexible Modeling System (FMS) GCM conserves angular momentum to better than 2% per 1000 Venus years ($\approx 225,000$ Earth days) of integration under the extreme conditions of a simplified Venus simulation with low surface torques.

With no topography in the GCM, physical torques due to surface/atmosphere frictional interactions dominate the acceleration of an initially stationary atmosphere and provide more than four times the angular momentum of solid body co-rotation over an integration period of 100 Venus years. During the subsequent steady state period of 200 Venus years negligible mean physical torques cause variation in the total angular momentum of less than 5% and produce a stable multi-century simulation. Diffusion and damping processes within the GCM account for AM losses of less than 0.2% per 1000 Venus years.

This study provides a stable comparison point for other GCMs by employing a simplified forcing scheme. The diagnostics and analysis require little or no modification to the core GCM and are sufficiently robust to allow easy model inter-comparison.

© 2012 Elsevier Inc. All rights reserved.

1. Introduction

Recent work with numerical models (Lebonnois, 2012; Parish et al., 2012) have suggested that under forcing conditions representative of the Venus atmosphere (e.g. Lee et al., 2007) some General Circulation Models (GCMs) do not conserve angular momentum (AM) well enough to realistically simulate super-rotating atmospheric circulation.

The results from Parish et al. (2012), for example, suggest that spurious numerical sources contribute significantly to the atmospheric AM in simplified setups, and only the introduction of stronger “more realistic” forcing from mountain torques reduces the measured errors sufficiently to simulate an atmospheric circulation dominated by physically attributable AM. In Lebonnois (2012) and Parish et al. (2012) the effect of numerical errors present in their models was mitigated by including realistic topography that in turn produces sufficiently large mountain torques to dominate the extant numerical errors.

We show in this paper that a state of the art Venus GCM based on the Geophysical Fluid Dynamics Laboratory (GFDL) Flexible Modeling System (FMS) is able to conserve AM over century-long integrations without topography and its associated mountain-torques, with an estimated non-conservation of AM of two percent per 1000 Venus years of simulation. During the 200 Venus years ($\approx 45,000$ Earth days) of steady-state simulation in this experiment, the intrinsic variability of the global AM is 5%, almost 10 times larger than the non-conservation losses.

This simulation is performed using the simplest configuration described in Lee et al. (2007) and shown by Lebonnois (2012) and Parish et al. (2012) to be problematic in their GCMs. In the next section we provide the context of this work and discuss briefly the results presented by Lebonnois (2012) and Parish et al. (2012). In Section 3 we discuss the methodology used in this study to measure the global AM conservation in the FMS Spectral GCM. In Section 4 we present simple and robust results from a multi-century simulation, and provide quantified measures of the long term AM non-conservation of the GCM. Finally, in Section 5 we provide a summary and our conclusions.

In the remainder of this text, *years* refers to Venus years, 225 Earth days in length. Where appropriate, the approximate number of Earth days is given for periods larger than 1 year.

2. Context for the experiment

Both Lebonnois (2012) and Parish et al. (2012) examined non-conservation of AM in their Venus GCMs. The first GCM is the National Centers for Atmospheric Research (NCAR) Community Atmosphere Model (CAM), modified for use as a Venus GCM at the University of California, Los Angeles (UCLA) (Parish et al., 2011). The second GCM is developed by the Laboratoire de Météorologie Dynamique (LMD) and the Institut Pierre-Simon Laplace (IPSL) (Lebonnois et al., 2010).

These GCMs are configured using the forcing described in Lee et al. (2007) (referred to by the authors as the “ISSI configuration”, Lebonnois et al. (2011)) with a simple linear relaxation scheme to represent the radiative forcing of the atmosphere (c.f. Held and Suarez, 1994) and a Rayleigh friction boundary layer that relaxes the surface layer winds to rest over multi-day time-scales. In this configuration diagnostics of the globally integrated atmospheric AM and torques are calculated as a function of time for various components of the GCM, including the planetary boundary layer, mountain torques, diffusive filters, and the dynamical core.

Using these diagnostics Lebonnois (2012) and Parish et al. (2012) show that the dynamical cores of their GCMs are non-conservative, both being strongly influenced by non-physical torques generated by the numerical components of their models. CAM is more non-conservative than the IPSL/LMD GCM, despite the higher horizontal resolution used in CAM. In the CAM GCM without topography (Parish et al., 2012) atmospheric angular momentum changes correlate almost completely with the dynamical-core torques, rather than the physical torques from the boundary layer scheme (their Fig. 1).

For a GCM simulation to produce meaningful results the angular momentum change in the atmosphere should be attributable to the physical boundary layer torques. As a result, non-conservation losses associated with numerical approximations and filtering should be limited to fractions of percent loss over typical integration timescales (centuries, for Venus). For the simplified FMS Venus GCM presented here, very small numerical errors contribute to an AM non-conservation rate of about two percent per 1000 years.

* Corresponding author.

E-mail address: lee@ashimaresearch.com (C. Lee).

3. Methodology

To examine AM conservation in the FMS Venus GCM we used the simplest possible experiment configuration (Lee et al., 2005, 2007; Lee and Richardson, 2010). This configuration is the same as that used by other groups (e.g. Herrnstein and Dowling, 2007) and the majority of experiments in the ISSI inter-comparison study (Lebonnois et al., 2011). As such, results from this experiment are applicable directly to the results of Lee and Richardson (2010) (using the same GCM) and provide a replicable comparison point for other simplified GCMs. A secondary reason for choosing such a simple configuration is that one major result from Parish et al. (2012) and Lebonnois (2012) is that the simplified configuration is particularly non-conservative in their GCMs. One proposed solution is to include topography in the model which induces pressure-gradient driven mountain torques and increases the (gross) global torques attributable to the boundary layer.

Starting with the Lee et al. (2007) configuration we include additional diagnostics of the AM contribution from the physical parameterizations and dynamical core, calculating diagnostic fields at the end of each model timestep. Torques from physical parameterizations are calculated directly by the GCM, while torques from the dynamical core are explicitly calculated from the change in the wind field (and hence AM) during the timestep. Specific angular momentum m (in $\text{m}^2 \text{s}^{-1}$) is calculated as

$$m = R \cos \phi (R\Omega \cos \phi + u), \quad (1)$$

where R is the planetary radius (in meters, assuming Venus is a sphere of radius 6,040,000 m), ϕ the planetocentric latitude, Ω the rotation rate (in radians/s), and u is the longitudinal wind. In comparison, specific AM tendencies are calculated as

$$\frac{\partial m}{\partial t} = R \cos \phi \frac{\partial u}{\partial t}, \quad (2)$$

where $\frac{\partial}{\partial t}$ is the rate of change in x with respect to time. The total atmospheric angular momentum M (in $\text{kg m}^2 \text{s}^{-1}$) is then calculated as the mass integral of the specific angular momentum m ,

$$M = \int m d\mu, \quad (3)$$

$$= \frac{1}{g} \int m R^2 \cos \phi d\phi d\lambda dP,$$

where μ is the mass of the air parcel with specific angular momentum m , λ is the longitude, g is the planetary gravitational acceleration (assumed constant at 8.87 m s^{-2}), and P is the atmospheric pressure (in Pascal).

In this study, we define AM contributions from the dynamical core $\tau_d = \frac{\partial M_d}{\partial t}$ and the physical parameterizations $\tau_p = \frac{\partial M_p}{\partial t}$, where the latter contains the explicit contributions from the Rayleigh friction boundary layer and the weak damping and the model top (the ‘‘sponge’’ layer; Lee et al., 2007). We additionally measure the total mass in the atmosphere and calculate the AM of the at-rest atmosphere M_0 as a function of time. The total AM can then be calculated as a time (t) integral of all torques and the initial total AM M_{initial} ,

$$M_t = M_{\text{initial}} + \int \left(\frac{\partial M_0}{\partial t} + \frac{\partial M_d}{\partial t} + \frac{\partial M_p}{\partial t} \right) dt. \quad (4)$$

Alternatively, the total angular momentum can be calculated directly from Eq. (3) for a given wind field, referred to here as M_c (and $\tau_c = \frac{\partial M_c}{\partial t}$).

Assuming that there should be no net torques from the dynamical core, we define an error term τ_e as the sum of the torques due to the change in atmospheric mass and the dynamical core,

$$\tau_e = \frac{\partial M_d}{\partial t} + \frac{\partial M_0}{\partial t}. \quad (5)$$

Numerically, the AM is calculated at each physical grid-point within the GCM and integrated vertically using the layer mass calculated at the time of the AM calculation. These column integrated values are output from the GCM and are globally integrated using the Climate Data Analysis Toolkit (CDAT, Doutriaux et al., 2009) to complete Eq. (3) (CDAT is used to calculate appropriate area weighting values using the bounding boxes defined by the GCM and to perform the area integration). The time integration in Eq. (4) is completed using a Trapezoidal rule. The values of M_t and M_c are essentially identical in this experiment (Fig. 1), suggesting that numerical time integration errors (performed only on M_t) are negligible. Numerical precision errors in the area integration may be present but affect all fields equally and cannot be disentangled with the current GCM configuration (an absolute ‘‘truth’’ value for the global AM is not known). These errors do not affect the conclusions of the experiment.

4. Results

We integrate the FMS Venus GCM from rest for 300 years ($\approx 70,000$ Earth days) in the configuration described in Lee and Richardson (2010). In this experiment the GCM uses a spectral element dynamical-core model with a triangular truncation at wavenumber 21 (T21). The physical resolution of the GCM is approximately 5.625° in longitude and latitude (64×32 grid points), and the model integration timestep is 120 S.I. (Earth) seconds.

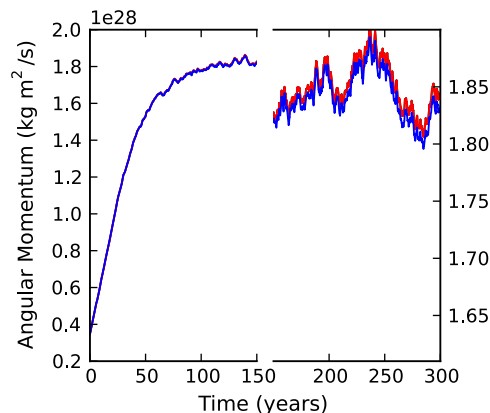


Fig. 1. Integrated angular momentum over 300 Venus years of simulation. (black, but entirely covered by red) Calculation of AM from the model wind field, M_c , (red) Integrated AM from the total change during each timestep M_t , (blue) Integrated AM from physics contributions M_p . The vertical axis changes scale after year 150. (For interpretation of the references to color in this figure legend, the reader is referred to the web version of this article.)

During the first 100 years of simulation the atmosphere gains more than $1.5 \times 10^{28} \text{ kg m}^2 \text{ s}^{-1}$ of AM, increasing the total atmospheric AM to a global Super-rotation of 5 (Read, 1986). For a 200 year period after year 100, the variation in total AM is about 5% of that total, with no net long term trend. The Venus GCM shows no secular decrease in angular momentum after an extended integration comparable to that shown by Lebonnois (2012).

Fig. 1 shows the AM calculated from the GCM from three different diagnostic fields. The first (black) is the total angular momentum M_t calculated directly from wind field (Eq. (3)); the second (red) is the integrated AM from Eq. (4), M_c ; the third (blue) is calculated from Eq. (4) using the physical torques only, omitting the contribution from the error term τ_e . In this experiment M_c matches exactly the integrated M_t and the corresponding lines in Fig. 1 overlap. The difference between the integrated physical torques M_p and the calculated M_c is approximately 0.6% at the end of the 300 year integration.

Fig. 2 shows the differential counterpart to Fig. 1. Showing the explicitly calculated change in AM from changes to the M_c field (τ_c , black), each differential term in Eq. (4), and also the contribution from explicit numerical damping within the dynamical core (already included in the dynamical core term τ_d). In this experiment τ_c and τ_p are almost the same and overlap significantly in this figure (blue and black lines in Fig. 2). The initial spin-up period of ~ 80 years is clearly visible as the period when integrated physical torques are almost always positive.

Fig. 3 shows the integrated contribution from τ_d , τ_0 , and the explicit diffusion, expressed as a percent of the total M_c . The mass-conservation term τ_0 contributes essentially nothing to the total error (parts per million of M_c), and damping causes a negative error (removing momentum). The majority of the error is attributable to the residual effect of the dynamical core τ_d . After 300 years, this error is 0.6% of the total AM, 10 times smaller than the variability during the last 200 years of

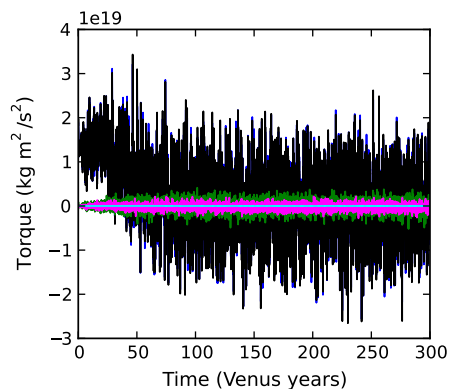


Fig. 2. Torque ($\frac{\partial M_c}{\partial t}$) on the model wind field and torques applied by the physical parameterizations and dynamical core. (black) calculated torque τ_c , (blue) physical torques τ_p , (green) dynamical core torque τ_d , (magenta) diffusive torques (included in green), (cyan) effective torque due to non-conservation of mass τ_0 (magnitudes are $10^{12} \text{ kg m}^2 \text{ s}^{-2}$). (For interpretation of the references to color in this figure legend, the reader is referred to the web version of this article.)

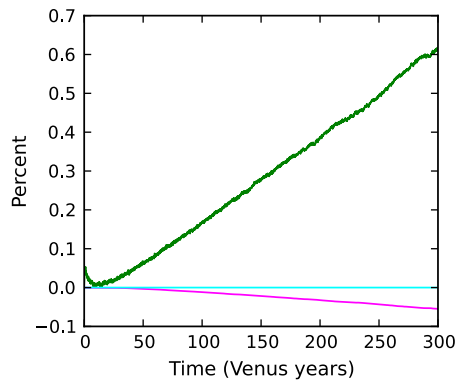


Fig. 3. Integrated momentum from the dynamical core M_d (green), from diffusion (magenta), and from mass non-conservation (cyan). All values are expressed as a fraction of the total angular momentum M_c (all as a function of time). (For interpretation of the references to color in this figure legend, the reader is referred to the web version of this article.)

simulation. The non-conservation error grows at a constant rate of about 2% per 1000 years. The constant growth in the error implies a constant (but noisy) error in the dynamical core calculations, in contrast to a large intermittent error that might appear with the build up and release of momentum within the numerical algorithms.

Physical torques are responsible for essentially all of the atmospheric AM change since the start of the integration. More than 99% of the AM after 300 years is attributable to the physical torques. If the residual error shown in Fig. 3 continue to grow, it would reach approximately 2% of total angular momentum after 1000 years, four times longer than a typical run in Lebonnois et al. (2011) and more than 10 times longer than the time required to initialize a steady state from rest with the Lee et al. (2007) configuration (95% of the AM is present after 96 years of simulation). Over the entire integration, physical torques (τ_p) apply an average of $2.344 \times 10^{18} \text{ kg m}^2 \text{ s}^{-2}$, compared to an actual rate of change ($\frac{\Delta M_c}{\Delta t}$) of $2.357 \times 10^{18} \text{ kg m}^2 \text{ s}^{-2}$. The dynamical core applies torques of $1.3 \times 10^{16} \text{ kg m}^2 \text{ s}^{-2}$.

The torque applied by the surface friction to the atmosphere in the GCM varies from a net positive input during the initial 'spin-up' to net zero input at steady-state (e.g. the last 200 years, Fig. 2). The spin-up phase being characterized by negative winds in the boundary layer leading to acceleration of the atmosphere ($\tau_p \propto -u$, Lee et al., 2007). As the mid-latitude jets gain momentum the lower atmosphere winds in the mid-latitudes become increasingly positive, reducing the net acceleration. Finally, in the steady-state circulation, the balance in the boundary layer is between the net acceleration in the equatorial region and the net deceleration in the mid-latitude regions of both hemispheres. Throughout the entire integration, including the steady-state (where net acceleration is essentially zero), the physical torques (τ_p) and the calculated changes in AM (τ_c) have a correlation coefficient of 98%, compared with a 17% correlation between the residual dynamical-core torques (τ_r) and the changes in τ_c . During this steady period the time-mean physical torque $\bar{\tau}_p = 1.9 \times 10^{16} \text{ kg m}^2 \text{ s}^{-2}$ and time-mean residual torque is $\bar{\tau}_r = 1.5 \times 10^{16} \text{ kg m}^2 \text{ s}^{-2}$, but the variability of the physical torques (the standard deviation of the last 150 years) is 6 times higher at $7.15 \times 10^{18} \text{ kg m}^2 \text{ s}^{-2}$ compared with $1.14 \times 10^{18} \text{ kg m}^2 \text{ s}^{-2}$ for the variance in the dynamical-core torque. (The variance in the total AM field given by M_c is $7.27 \times 10^{18} \text{ kg m}^2 \text{ s}^{-2}$.) The mean absolute torque applied by the physical parameterizations during this time is $|\bar{\tau}_p| = 5.72 \times 10^{18} \text{ kg m}^2 \text{ s}^{-2}$ compared with the mean dynamical-core torque of $|\bar{\tau}_c| = 8.97 \times 10^{17} \text{ kg m}^2 \text{ s}^{-2}$ (in line with the correlation coefficients above).

During the last 150 years, M_c has a value of $1.850(\pm 0.020) \times 10^{28} \text{ kg m}^2 \text{ s}^{-1}$ (where the parenthetical value gives the standard deviation) and the mean residual torques applied to the atmosphere are $1.5(\pm 89) \times 10^{16} \text{ kg m}^2 \text{ s}^{-2}$, almost 10^{-12} times smaller. This number (10^{-12}) is almost four orders of magnitude larger than smallest (fractional) number representable by double precision numbers used in this GCM (i.e. 10^{-16} , fractional numbers smaller than this would be lost in any calculation). Errors in the spherical harmonic and Fourier transforms can produce errors in double precision numbers of 10^{-14} (Reinecke, 2010) or larger depending on the implementation, which might account for some of the error here. Summation errors inside the GCM and approximations made outside the GCM in analysis scripts also occur on the order of 10^{-14} or larger when calculating global sums or averages, and they would also cause errors in τ_c of similar size. Neither of these numerical considerations account for all of the residual dynamical-core torque.

A few potential sources of error remain. Approximations made within the Navier-Stokes equations for the discretized grid, in particular terms involving differentials, could account for some error and Parish et al. (2012) noted that decreasing the resolution of CAM increases their errors. Filtering of the time-integration equation (Robert, 1966; Asselin, 1972) within the FMS leapfrog scheme can cause conservation errors (Marsaleix et al., 2012). Violation, or near violation of stability constraints (e.g. the Courant-Friedrichs-Lewy, or CFL, criterion) will also cause

some losses due to 'overshoots' in the advection and transport algorithms. Some of these errors might be mitigated by reducing the timestep, but there is a numerical lower limit imposed on the timestep by the requirement that any change in the atmospheric fields be a representable fraction of the atmospheric field, i.e. a fractional change smaller than 10^{-16} will be lost because of the finite resolution of the floating point number representation used.

5. Conclusions

The results from this experiment are counter to the suggestion by Lebonnois (2012) and Parish et al. (2012) of a fundamental non-conservation of AM in recent simplified Venus GCM simulations (e.g. Lebonnois et al., 2011; Lee et al., 2007). Both suggested that the simplified forcing alone was insufficient to produce a realistic atmospheric state with their GCMs. We have shown in an integration of the simplified FMS Venus GCM (Lee and Richardson, 2010) that angular momentum is conserved to a rate of better than 2% per 1000 years, with 98% of the angular momentum being directly attributable to the torques applied through the lower boundary layer. The longest integrations used in recent publications are the multi-century integrations in Lebonnois et al. (2011) (the "ISSI inter-comparison"), too short for numerical non-conservation to have a significant impact in the FMS Venus GCM. This result satisfies a fundamental requirement for GCMs that is necessary before more advanced physical forcing can meaningfully be examined in Venus models.

One possible source of non-conservation explored by Parish et al. (2012) is the implementation of diffusion and damping in their GCM. In similar tests with the FMS spectral core investigated here, this component of the model actually removes angular momentum from the system, at a rate of almost 0.2% per 1000 years. It only accounts for a small fraction of the AM non-conservation found in our GCM and does not increase the total AM in this experiment.

The FMS Venus GCM experiment was conducted with the simplest possible configuration. During spin-up of the GCM, the physical torques clearly dominate all other torques in the GCM, and they are the only torques to have non-zero net effect on the GCM within their intrinsic variability. During the steady-state part of the integration the time-mean absolute value and variance of the physical torques are significantly higher than the residual torques and dominate the actual changes in atmosphere AM reservoir as calculated from τ_c .

In contrast, the GCM simulations described by Lebonnois (2012) and Parish et al. (2012) used topography to introduce additional physical torques that help mitigate the effect of residual numerical errors. Proper representation of topographic forcing must be a goal of more complete Venus GCMs, but the inclusion of topography is not a useful method to correct any non-conservation errors in a GCM. Adding topography generates additional physical acceleration of the boundary layer wind fields and may overwhelm the conservation errors in a GCM, but it does not address the underlying numerical non-conservation present in the GCM. Even with topography, rigorous long term diagnostics would be needed to determine the contribution of the residual dynamical-core errors.

Acknowledgments

This work was carried out under NASA PATM Grant NNX11AD94G. Resources supporting this work were provided by the NASA High-End Computing (HEC) Program through the NASA Advanced Supercomputing (NAS) Division at Ames Research Center. We are grateful to the two anonymous reviewers whose comments have helped clarify and improve this manuscript.

References

- Asselin, R., 1972. Frequency filter for time integrations. *Mon. Weather Rev.* 100, 487–490.
- Doutriaux, C., Drach, R., McCoy, R., Mlaker, V., Williams, D., 2009. Climate data analysis tools facilitate scientific investigations. *Eos Trans. AGU* 90 (35), 297. doi:10.1029/2009EO350002.
- Held, I., Suarez, M., 1994. A proposal for the intercomparison of dynamical cores of atmospheric General Circulation Models. *Bull. Am. Meteorol. Soc.* 75 (10), 1825–1830. <http://www.gfdl.gov/bibliography/related_files/ih9401.pdf>.
- Herrnstein, A., Dowling, T.E., 2007. Effects of topography on the spinup of a Venus atmospheric model. *J. Geophys. Res.* – Planets 112 (E4), 1–9. <http://www.agu.org/pubs/crossref/2007/2006JE002804.shtml>.
- Lebonnois, S., 2012. The mechanism of superrotation in Venus and Titan LMD GCM. *Comp. Climatol. Terr. Planets*, 1–2. <http://www.lpi.usra.edu/meetings/climatology2012/pdf/8004.pdf>.
- Lebonnois, S., Hourdin, F., Eymet, V., Cresspin, A., Fournier, R., Forget, F., 2010. Superrotation of Venus' atmosphere analyzed with a full General Circulation Model. *J. Geophys. Res.* 115 (E6), E06006.
- Lebonnois, S., Lewis, S.R., Yamamoto, M., Lee, C., Dawson, J., Read, P.L., Mendonca, J., Parish, H., 2011. *Geophys. Res. Abstracts*, 13, EGU2011-6293.
- Lee, C., Richardson, M.I., 2010. A General Circulation Model ensemble study of the atmospheric circulation of Venus. *J. Geophys. Res.* – Planets 115 (E4), E04002.
- Lee, C., Lewis, S.R., Read, P.L., 2005. A numerical model of the atmosphere of Venus. *Adv. Space Res.* 36 (11), 2142–2145. doi:10.1016/j.asr.2005.03.120.

- Lee, C., Lewis, S.R., Read, P.L., 2007. Superrotation in a Venus General Circulation Model. *J. Geophys. Res. – Planets* 112 (E04S11), 1–10.
- Marsaleix, P., Auclair, F., Duhaut, T., Estournel, C., Nguyen, C., Ulses, C., 2012. Alternatives to the Robert–Asselin filter. *Ocean Model.* 41, 53–66.
- Parish, H.F., Schubert, G., Covey, C., Walterscheid, R.L., Grossman, A., Lebonnois, S., 2011. Decadal variations in a Venus General Circulation Model. *Icarus* 212 (1), 42–65.
- Parish, H.F., Lebonnois, S., Schubert, G., Covey, C., Walterscheid, R.L., Grossman, A., 2012. Importance of the angular momentum budget in Venus atmosphere General Circulation Models. *Comp. Climatol. Terr. Planets*, 1–2, <<http://www.lpi.usra.edu/meetings/climatology2012/pdf/8017.pdf>>.
- Read, P.L., 1986. Super-rotation and diffusion of axial angular momentum: I. “Speed limits” for axisymmetric flow in a rotating cylindrical fluid annulus. *Q. J. R. Meteorol. Soc.* 112, 23–251.
- Reinecke, M., 2010. Libpsht – Algorithms for efficient spherical harmonic transforms. *Astron. Astrophys.* 526 (A109), 1–9.
- Robert, A.J., 1966. The integration of a low order spectral form of the primitive meteorological equations. *J. Meteorit. Soc. Jpn.* 44, 237–245.